

A new Bioelectrochemical Method for Detect Nitrite (NO_2^-) and Hydroxylamine (NH_2OH) by Using of Hydroxylamine Oxidase (HAO) and Modified Electrode with Zirconia Nanoparticles

Hamideh Dehghani¹, Mahnaz Bezhgi², Roya Malekzadeh², Elahe Imani², Saeid Pasban-Noghabi³, Gholamreza Javadi⁴, Reza Faraji⁵, Masoud Negahdary⁶, Reza Aghebati-Maleki^{7,*}

¹ Department of Nursing, Shahid Sadoughi University of medical sciences, Yazd, Iran

² Department of Biology, Payame Noor University, I.R. of IRAN

³ Bsc in anesthesia, student research committee, Gonabad University of medical sciences, Gonabad, Iran

⁴ Department of Endodontic, Shahid Sadoughi University of medical sciences, Yazd, Iran

⁵ Department of Microbiology, Faculty of medicine, Kermanshah University of medical sciences, Kermanshah, Iran

⁶ Yazd Cardiovascular Research Center, Shahid Sadoughi University of Medical Sciences, Yazd, Iran

⁷ Immunology Research Center, Tabriz University of Medical Sciences, Tabriz, Iran

*E-mail: Reza.Aghebati@yahoo.com

Received: 18 October 2013 / Accepted: 29 November 2013 / Published: 5 January 2014

To design a new bioelectrochemical method to detect Nitrite (NO_2^-) and hydroxylamine (NH_2OH) employing Hydroxylamine oxidase (HAO) and modified electrode by Zirconia Nanoparticles (ZrO_2 NPs) we benefited the bioelectrochemical methods. The morphological studies of Zirconia Nanoparticles were carried out by atomic force microscope (AFM), transmission electron microscope (TEM), X-ray diffraction (XRD) and TU-1901 double-beam UV-visible spectrophotometer (UV-VIS). Electrochemical studies were done by cyclic voltammetry (CV) method. The formal potential (E^0) for the HAO redox reaction on the HAO / ZrO_2 NPs/ carbon paste electrode (CPE) was 250 mV with respect to the reference electrode (SCE). The final results show the linear dependence of the anodic peak current on the NO_2^- concentration in the range of 3 to 117 μM . The stability of HAO / ZrO_2 NPs/CPE electrode biosensor has been checked by carrying out the experiments at the regular interval of a week and it has been found that HAO / ZrO_2 NPs/CPE electrode based biosensor retains its 87% activity after 21 days.

Keywords: bioelectrochemistry, Nitrite, hydroxylamine, Hydroxylamine oxidase, Zirconia Nanoparticles

1. INTRODUCTION

Nanostructures display unique mechanical, electrical, chemical, and optical properties. Nanotechnology is an area of science that involves working with materials and devices on a nanoscale level. On scalable terms, a nanometer is approximately 1/80,000 of the diameter of a human's hair, or 10 times smaller than the diameter of a Hydrogen atom[1-2]. Its functions are expanded across all areas of sciences including physics, chemistry, and biology. The name "nanotechnology" is used to summarize a wide range of very varied innovations and developments[3-5]. The common feature of all these technologies is the comparatively small size of the mechanical or electronic components produced, as well as that of objects made from very different chemical elements and compounds[6]. Nanotechnology is characteristically diverse in its potential applications, and offers the potential for completely new products and applications right across the board in all industries[7]. These special features of nanomaterial are used in designing new biosensors. Biosensor is a device that consists of two main parts: A bioreceptor and a transducer[8-9]. Bioreceptor is a biological component (tissues, microorganisms, organelles, cell receptors, enzymes, antibodies, nucleic acids, etc) that recognizes the target analyte. The other part is transducer, a physicochemical detector component that converts the recognition event into a measurable signal [10]. The function of a biosensor depends on the biochemical specificity of the biologically active material. Potentiometric Biosensors that we designed a novel case of it, are the least common of all biosensors, but different strategies may be found nonetheless in potentiometric Biosensors in which the measured parameter is oxidation or degrading the potential of an electrochemical reaction[11-12]. The function principle relies on the fact that when a voltage is applied to an electrode in solution, a current flow occurs because of electrochemical reactions. The voltage, at which these reactions occur, indicates a particular reaction and particular species. In these biosensors, direct electron transfer between redox proteins and electrodes is of practical and theoretical interest and can be improved by electrode or protein modification[13]. Zirconia nanoparticles that our research team used in this study are of great interest due to their improved optical, electrochemical and electronic properties with applications as piezoelectric, electro-optic and dielectric materials[14]. Zirconia is also emerging as an important class of catalyst[15]. The synthesis of zirconia has been realized by physico-chemical methods such as sol-gel synthesis, aqueous precipitation, thermal decomposition and hydrothermal synthesis. The study of NO reducing enzymes or their cofactors adsorbed on electrodes can provide important insights over the factors that control selectivity in NO reduction by enzymes and inorganic catalysts. In these systems the oxidation state of the enzyme or its cofactor can be directly controlled by the potential applied to the electrode[16]. Catalytic reaction steps are widely used in the chemical industry. By the contribution of nanoscale catalysts, the consumption of raw materials can be significantly reduced and side reactions as well as energy consumption can be minimized. Enzymes catalyze a wide variety of reactions that enable vital biological processes such as respiration, processing of food, structure of organs and photosynthesis. Most enzymes are proteins, which are the complex organic molecules made from amino acids[17]. The catalytic reaction occurs at a particular place in the enzyme, the so-called active site. At this place the reacting molecules interact with the enzyme. The high activity and selectivity of enzymes has always encouraged the mankind to use them as the catalysts in industrial processes.

Enzymes that catalyze redox reactions are called redox enzymes (e.g., Hydroxylamine oxidase in this study). In order to activate the redox enzyme, the electrons have to be transported to or from the enzyme[18]. Natural processes make use of so-called electron donors and acceptors, which are relatively large molecules. These molecules are expensive and it is generally not economically feasible to use them in industrial processes. However, if the enzyme is immobilized on a conducting support, this support can function as an electron source or drain, removing the necessity to use electron donors and acceptors[19-20]. The structure of Nitrite, hydroxylamine and Hydroxylamine oxidase are shown in figure 1 (a), (b) and (c), respectively.

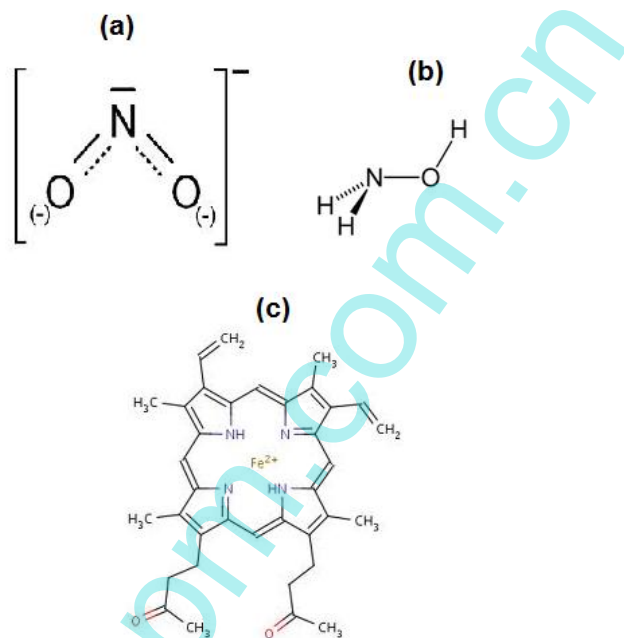


Figure 1. Structure of (a): Nitrite, (b): hydroxylamine and (c): Hydroxylamine oxidase

In this paper, we investigated the electrochemical behavior of Hydroxylamine oxidase enzyme by use of carbon paste electrode (CPE) and Zirconia nanoparticles and also the redox reactions of mentioned electrochemical behavior used as NO_2^- and NH_2OH biosensor.

2. EXPERIMENTAL

2.1. Materials

Hydroxylamine, Hydroxylamine oxidase, Zirconyl chloride octahydrate and Nitrite were purchased from sigma-aldrich and other chemicals used were purchased from Merck Company. Phosphate buffer solutions (PBS, 0.1M) with various pH values were prepared by mixing the stock standard solutions of Na_2HPO_4 and NaH_2PO_4 and adjusting the pH with H_3PO_4 or NaOH . All other chemicals were of analytical grade and all the solutions were prepared with doubly distilled water.

2.2. Apparatus

Surface morphological studies were carried out using Being Nano-instruments CSPM4000, atomic force microscope (AFM) and transmission electron microscope (TEM) measurement was conducted by using a DS-720 (Topcon Co. Ltd.), respectively. Cyclic voltammetry (CV) and square wave voltammetry were performed using an Autolab potentiostat PGSTAT 302 (Eco Chemie, Utrecht, The Netherlands) driven by the General purpose Electrochemical systems data processing software (GPES, software version 4.9, Eco Chemie). Electrochemical cell with three electrodes was used [21]; unmodified carbon paste electrode or carbon paste electrode modified with zirconia Nanoparticles was used as a working electrode, saturated calomel electrode (SCE) was used as a reference electrode while the platinum wire applied as a counter electrode. The phase characterization of ZrO_2 nanoparticles was performed by means of X-ray diffraction (XRD) using a D/Max-RA diffractometer with $CuK\alpha$ radiation. The absorbance properties of prepared nanoparticles were measured and recorded employing a TU-1901 double-beam UV-visible spectrophotometer.

2.3. Synthesis of ZrO_2 Nanoparticles

The ZrO_2 nanoparticles were prepared according to the literature. Initially, 2.58 g $ZrOCl_2 \cdot 8H_2O$ and 4.80 g urea were dissolved in 20.0 mL CH_3OH under stirring to form a colorless solution. The solution was transferred to a 20-mL Teflon-lined stainless steel autoclave, which was heated to 200 °C and retained at which for 20 h. The obtained white product was post-treated with sulphuric acid solution (0.167 mmol), and then calcined at 645 °C.

2.4. Preparation of unmodified carbon paste electrode (CPE) and modified CPE with zirconia Nanoparticles

Unmodified carbon paste electrode was prepared by mixing of 65% graphite powder and 35% paraffin wax. Paraffin wax was heated till melting and then, mixed appropriately with graphite powder to generate a homogeneous paste. The obtained paste was then packed into the bottom of an insulin syringe (i.d.: 2mm). External electrical contact was established by forcing a copper wire down the syringe. CPE modified with zirconia Nanoparticles was prepared by mixing 60% graphite powder and 30% paraffin wax with and 10% zirconia Nanoparticles. The surface of the electrode was polished with a piece of weighting paper and then rinsed with distilled water thoroughly.

2.5. Preparation of HAO- ZrO_2 Nps modified CPE

The modified electrode produced in previous section was used for production of HAO- ZrO_2 nanoparticles modified carbon paste electrode. In this section, the HAO was immobilized by dropping 5 μ l of 10 mg/ml of the enzyme solution onto the ZrO_2 nanoparticles modified carbon paste electrode and dried for about 30 min at room temperature. The electrode was then gently washed with deionized double distilled water and put at 4 °C when not in use.

3. RESULTS AND DISCUSSION

3.1. Microscopic characterization

As it is well known, the properties of a broad range of materials and the performance of a large variety of devices depend strongly on their surface characteristics. For instance, the surface of a biomaterial/biomedical device meets the physiological environment, immediately after it is placed in the body or bloodstream and the initial contact regulates its subsequent performance [22]. The average diameter of the synthesized ZrO_2 nanoparticle was between 20-35 nm, and has a very narrow particle distribution. This statement illustrated in figure 2. Figure 2 Shows a TEM image of ZrO_2 nanoparticles with 20 nm scale bare.

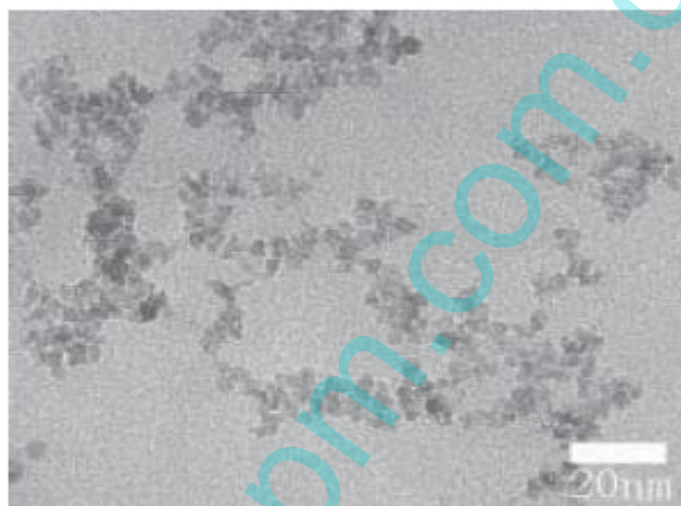
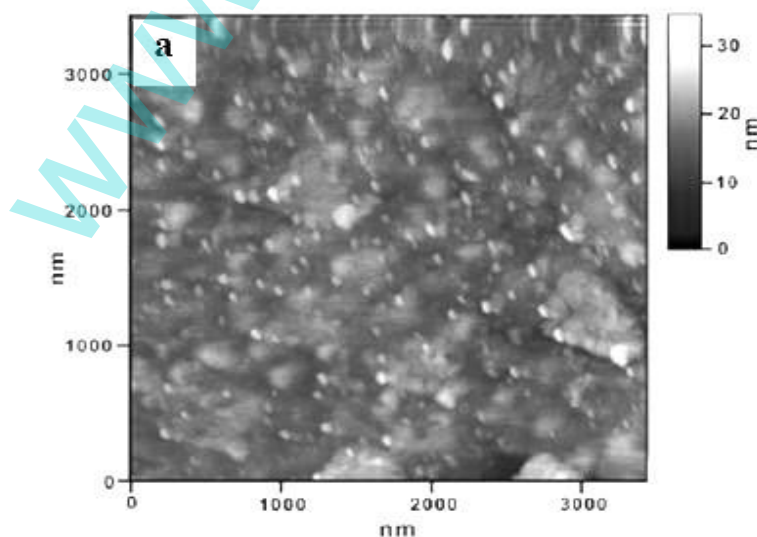


Figure 2. TEM images of ZrO_2 NPs, with diameter about 20 nm



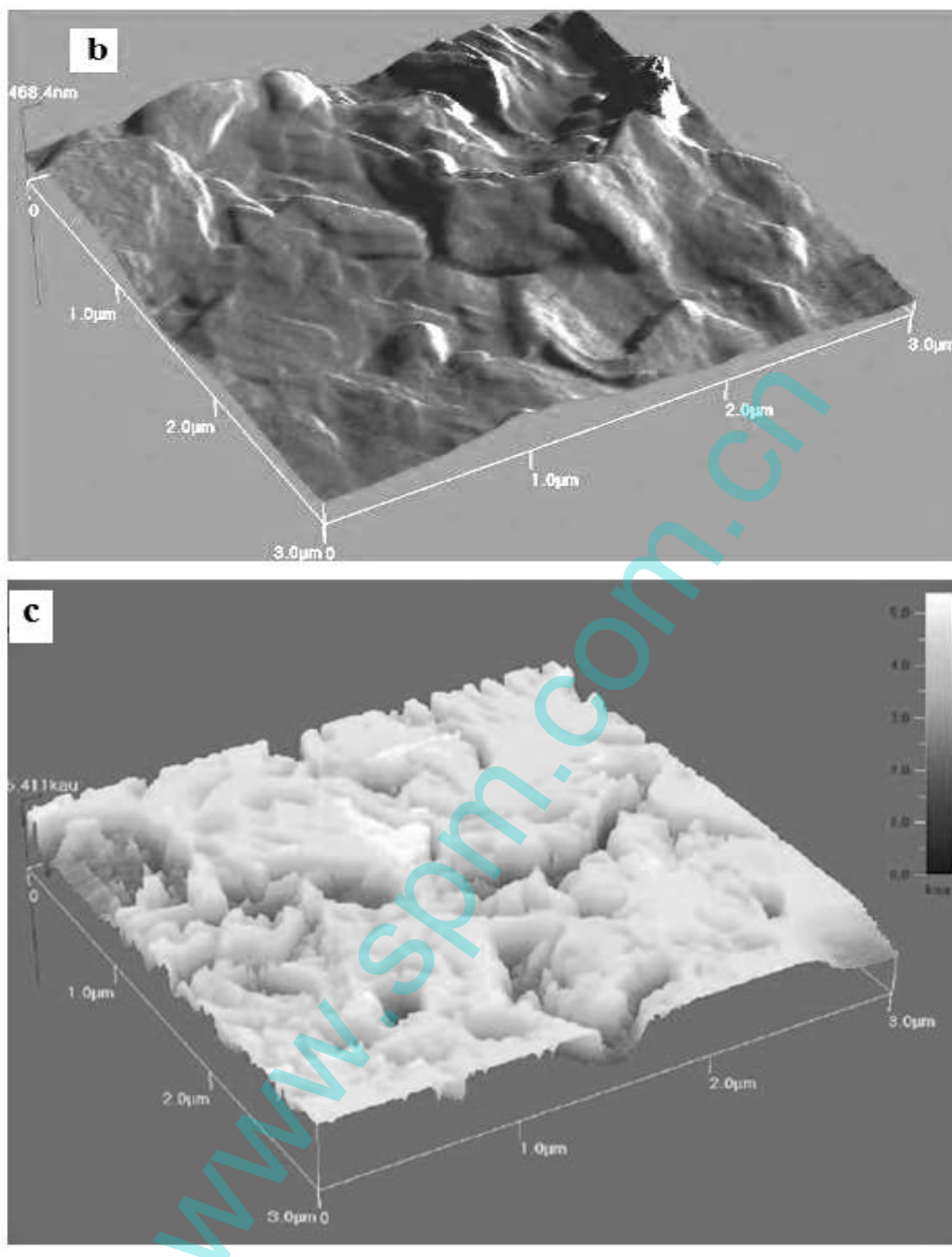


Figure 3. AFM images of (a) ZrO₂ NPs, (b) 3D Wave Mode AFM image of a bare CPE, 3 μm × 3 μm, z-scale 468 nm, scan frequency 1 Hz, And (c) AFM Phase Mode scans of a carbon paste electrode modified with zirconia Nanoparticles.

In the next study, initially synthesized zirconia nanoparticles were studied with atomic force microscope (AFM), that is shown in figure 3 (a). then bare Carbon paste electrode and Carbon paste electrode modified with zirconia nanoparticles were studied by atomic force microscope (AFM), that shown in figure 3 (b) and figure 3 (c), respectively.

3.2. X-Ray diffraction of ZrO₂ nanoparticles

The XRD pattern for ZrO₂ nanoparticles shown in Figure 4, the diffraction peaks are absorbed at 2θ values. The prominent peaks have been utilized to estimate the grain size of sample with the help of Scherrer equation [23] $D = K\lambda/(\beta \cos \theta)$ where K is constant (0.9), λ is the wavelength ($\lambda = 1.5418 \text{ \AA}$) (Cu $K\alpha$), β is the full width at the half-maximum of the line and θ is the diffraction angle. The grain size estimated using the relative intensity peak for ZrO₂ nanoparticles was found between 20-35 nm and the increase in sharpness of XRD peaks indicates that particles are in crystalline nature. All different peaks in figure 4 are related to ZrO₂ nanoparticles and matched to Joint Committee for Powder Diffraction Studies (JCPDS).

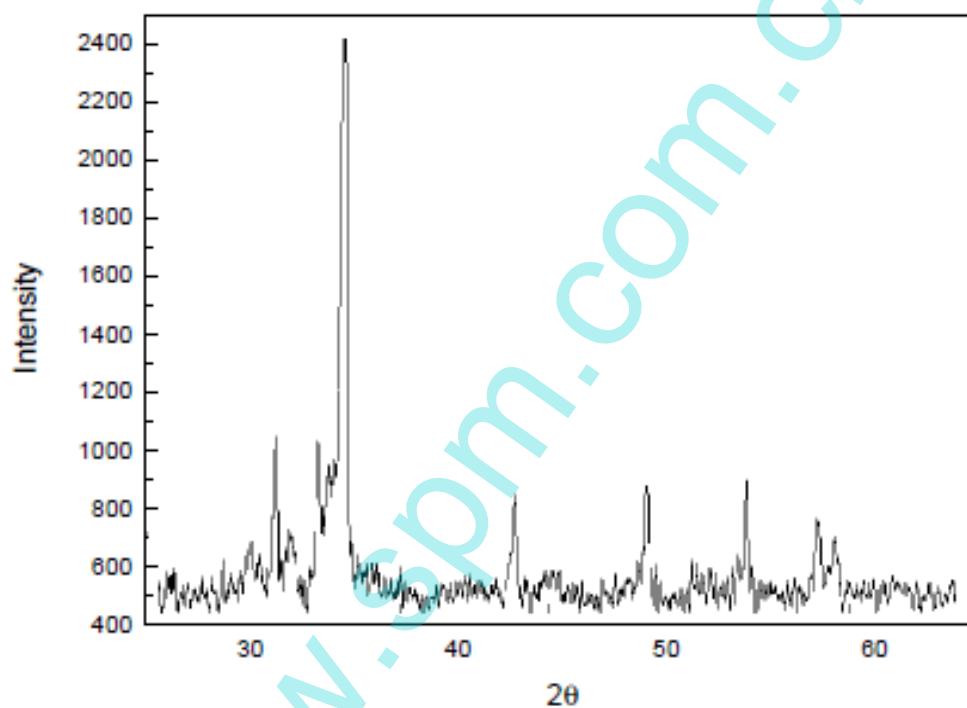


Figure 4. XRD pattern for ZrO₂ nanoparticles

3.3. UV-visible absorption spectra for ZrO₂ nanoparticles

The most dramatic property of nanoparticles is the size evolution of the optical absorption spectra. Hence, UV-visible absorption spectroscopy is an efficient technique to monitor the optical properties of quantum-sized particles. The UV-visible absorption spectra of ZrO₂ nanoparticles was shown in Figure 5; although the wavelength of our spectrometer is limited by the light source, the absorption band of the ZrO₂ nanoparticles have been shown a blue shift due to the quantum confinement in sample compare with bulk ZrO₂ particles. This optical phenomenon indicates that these nanoparticles show the quantum size effect [24].

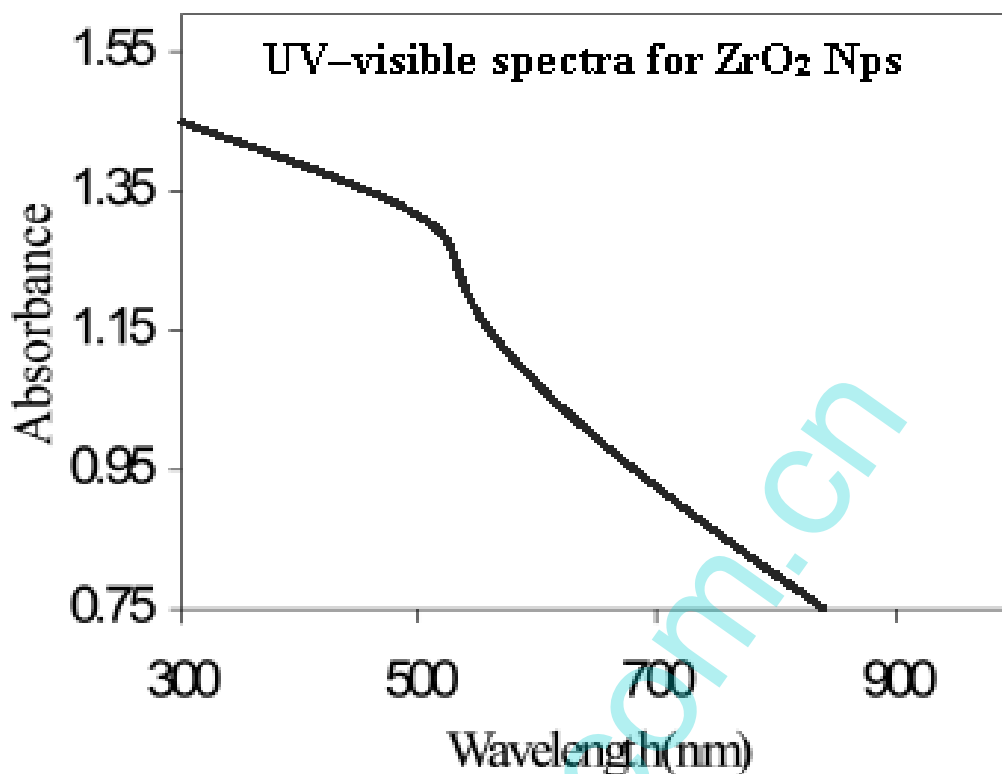


Figure 5. UV-Vis absorption spectra for ZrO₂ nanoparticles.

3.4. Direct electrochemistry of HAO / ZrO₂ nanoparticles /carbon paste electrode

The integrity of the immobilized Hydroxylamine oxidase construction and its ability to exchange electrons with the nanometer- scale ZrO₂ particles surfaces were assessed by voltammetry. A macroscopic electrode was required to attain a large enough Hydroxylamine oxidase sample to yield detectable direct oxidation and reduction currents. The comparative CVs for the ZrO₂ NPs/CPE and HAO / ZrO₂ NPs/ CPE in 0.1 M PBS (pH 7.0) was obtained. These voltammograms are demonstrated in Figure 6 (a, b). By this Figure, it was noticed that there was no voltammetric response on ZrO₂ NPs/carbon paste electrode (Figure. 6 (a)), which, Figure. 6 (b) depicts a well-defined pair of oxidation–reduction (redox) peaks, observed on the HAO / ZrO₂ NPs/ CPE at 100 mv/s scan rate value. The HAO / ZrO₂ NPs/ CPE presented the reductive peak potential at +200 mV and the corresponding oxidative peak potential at +300 mV (at 100 mV s⁻¹), illustrating the adsorbed Hydroxylamine oxidase on the nanometer-scale ZrO₂ nanoparticles surfaces. The difference of anodic and cathodic peak potential values was $\Delta E = 100$ mV. These redox peaks were attributed to the redox reaction of the Hydroxylamine oxidase electroactive center. The formal potential (E^0) for the Hydroxylamine oxidase redox reaction on the HAO / ZrO₂ NPs/ CPE was 250 mV with respect to the reference electrode (SCE).

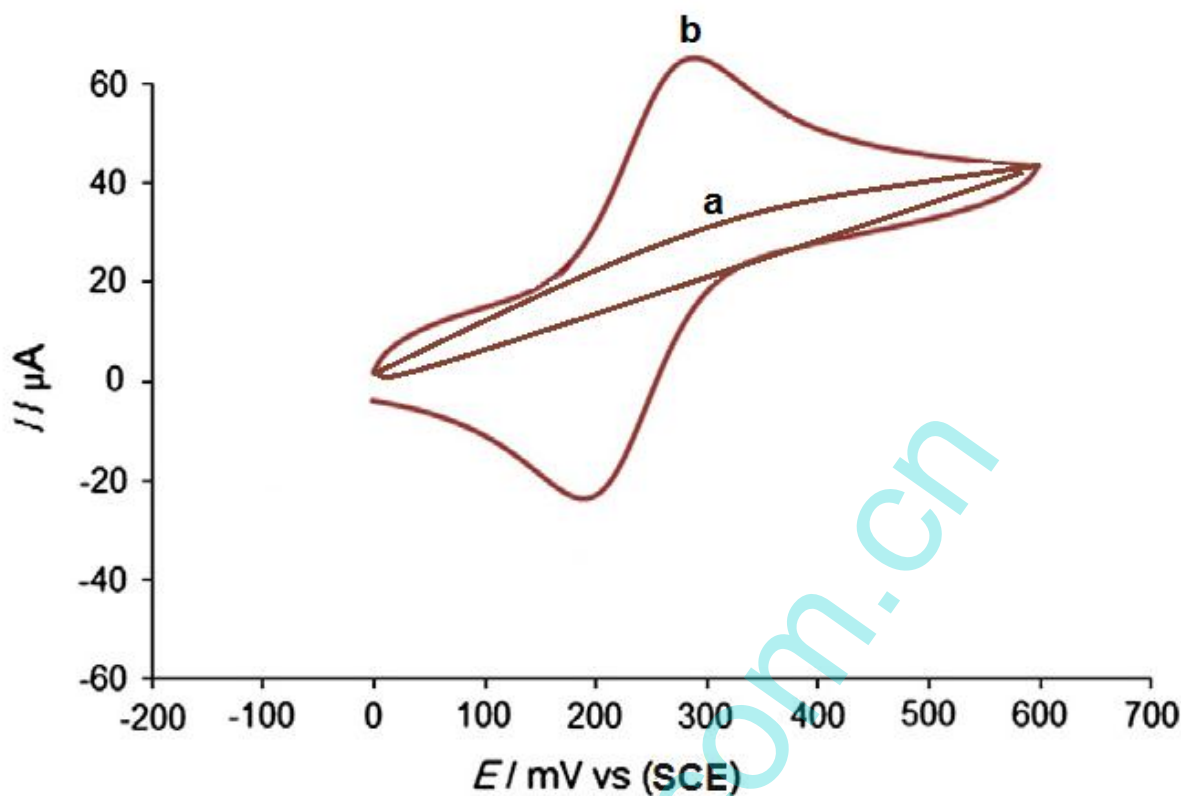


Figure 4. Cyclic voltammograms, using (a) the $\text{ZrO}_2\text{NPs/CPE}$ in 0.1 M phosphate buffer solution (PBS) and (b) $\text{HAO / ZrO}_2\text{ NPs/ CPE}$ in 0.1 M PBS (scan rate: 100 mV/s).

The collected cyclic voltammograms (CV) in Figure 5 (a) validated this statement that the nanometer-scale ZrO_2 NPs could play a key role in the observation of the Hydroxylamine oxidase CV facility response. On the grounds that the surface-to-volume ratio increases with the size degradation and because of the fact that the enzyme size is comparable with the nanometer-scale building blocks, these nanoparticles displayed a great effect on the electron exchange assistance between Hydroxylamine oxidase and carbon paste electrode. To further investigate the Hydroxylamine oxidase characteristics at the $\text{HAO / ZrO}_2\text{ NPs/ CPE}$ electrode, the effect of scan rates on the Hydroxylamine oxidase voltammetric behavior was studied in detail. The baseline subtraction procedure for the cyclic voltammograms was obtained in accordance with the method reported by Bard and Faulkner [25]. The scan rate (v) and the square root scan rate ($v^{1/2}$) dependence of the heights and potentials of the peaks are plotted in Figure 5 (b) and 5 (c). It is obvious that the redox peak currents increased linearly with the scan rate, the correlation coefficient was 0.985 ($i_{pc} = -0.5539v - 20.559$) and 0.9989 ($i_{pa} = +0.4735v + 21.996$), respectively. This phenomenon suggested that the redox process was an adsorption-controlled and the immobilized Hydroxylamine oxidase was stable. It can be seen that the redox peak currents increased more linearly with the v in comparison to that of $v^{1/2}$.

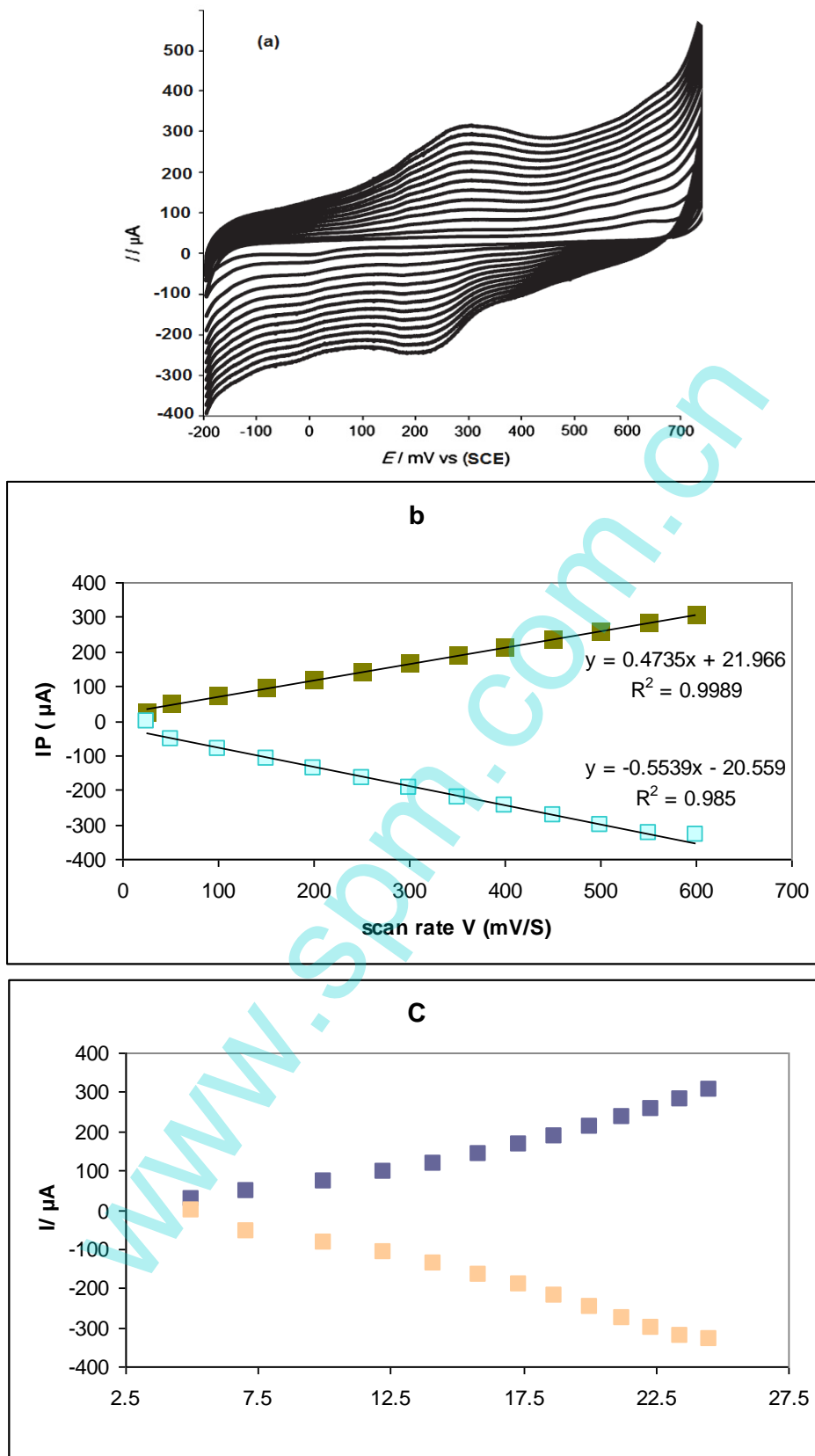


Figure 5. (a) CVs of HAO / ZrO₂ NPs/ CPE electrode in PBS at various scan rates, from inner to outer; 25, 50, 100, 150, 200, 250, 300, 350, 400, 450, 500, 550 and 600 mV s^{-1} , the relationship between the peak currents (i_{pa} , i_{pc}) vs., (b) the sweep rates and (c) the square root of sweep rates.

However, there is clearly a systematic deviation from linearity in this data, i.e., low scan rates are always on one side of the line and the high scan rate points are on the other. The anodic and cathodic peak potentials are linearly dependent on the logarithm of the scan rates (v) when $v > 1.0 \text{ V s}^{-1}$, which was in agreement with the Laviron theory, with slopes of $-2.3RT/\alpha nF$ and $2.3RT/(1-\alpha)nF$ for the cathodic and the anodic peak, respectively. So, the charge-transfer coefficient (α) was estimated as 0.51. Furthermore, the heterogeneous electron transfer rate constant (k_s) was estimated according to the following equation:

$$\left[\log k_s = \alpha \log(1-\alpha) + (1-\alpha) \log \alpha - \log \frac{RT}{nFv} - \frac{\alpha(1-\alpha)nF\Delta E_p}{2.3 RT} \right] \quad (1)$$

Here, n is the number of transferred electrons at the rate of determining reaction and R , T and F symbols having their conventional meanings. R , F and T are gas constant, Faraday constant and absolute temperature, respectively, all having definite values:

$$R = 8.314 \text{ J mol}^{-1} \text{ K}^{-1}, \quad F = 96493 \text{ C/mol}, \quad T = 298 \text{ K}$$

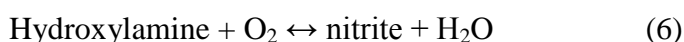
ΔE_p is the peak potential separation, giving an average heterogeneous transfer rate constant (k_s) value of 1.77 s^{-1} .

3.5. Electrocatalysis of HAO / ZrO₂ NPs/ CPE for detect NO₂⁻ and NH₂OH

Upon the addition of NO₂⁻ to 0.1M pH 7.0 PBS, the cyclic voltammogram of the HAO / ZrO₂ NPs/CPE electrode for the direct electron transfer of Hydroxylamine oxidase changed dramatically with an increase in oxidation peak current and a decrease in reduction peak current (Figure 6 (a)), while the change of cyclic voltammogram of bare or ZrO₂ NPs/ CPE was negligible (not shown), displaying an obvious electrocatalytic behavior of the Hydroxylamine oxidase to the reduction of NO₂⁻. The decreases of the reductive peak current were accompanied with the increases of the oxidative of HAO / ZrO₂ NPs/CPE. The electro-catalytic process could be expressed as follows:



In enzymology, a hydroxylamine oxidase (EC 1.7.3.4) is an enzyme that catalyzes the chemical reaction:



Thus, the two substrates of this enzyme are hydroxylamine and O₂, whereas, two products of which are nitrite and H₂O [8-12]. The heme pairs function as redox centers in electron transfer Mid-

point potentials have not been assigned to specific hemes [8-13]. This enzyme belongs to the family of oxidoreductases, specifically those acting on other nitrogenous compounds as donors with oxygen as acceptor [7-9]. For each turnover of hydroxylamine oxidase, one molecule of hydroxylamine is oxidized to nitrite, with the associated four electrons being transferred to the Quinone pool. Half of the achieved quinoas transfer electrons to the ammonia mono-oxygenase so that one molecule of hydroxylamine is generated from each molecule of ammonia [11-12]. The calibration curve (Figure 6 b) shows the linear dependence of the anodic peak current on the NO_2^- concentration in the range of 3 to 117 μM . In Figure 6 (b), at higher concentration of NO_2^- , the anodic peak current decreased and remained constant.

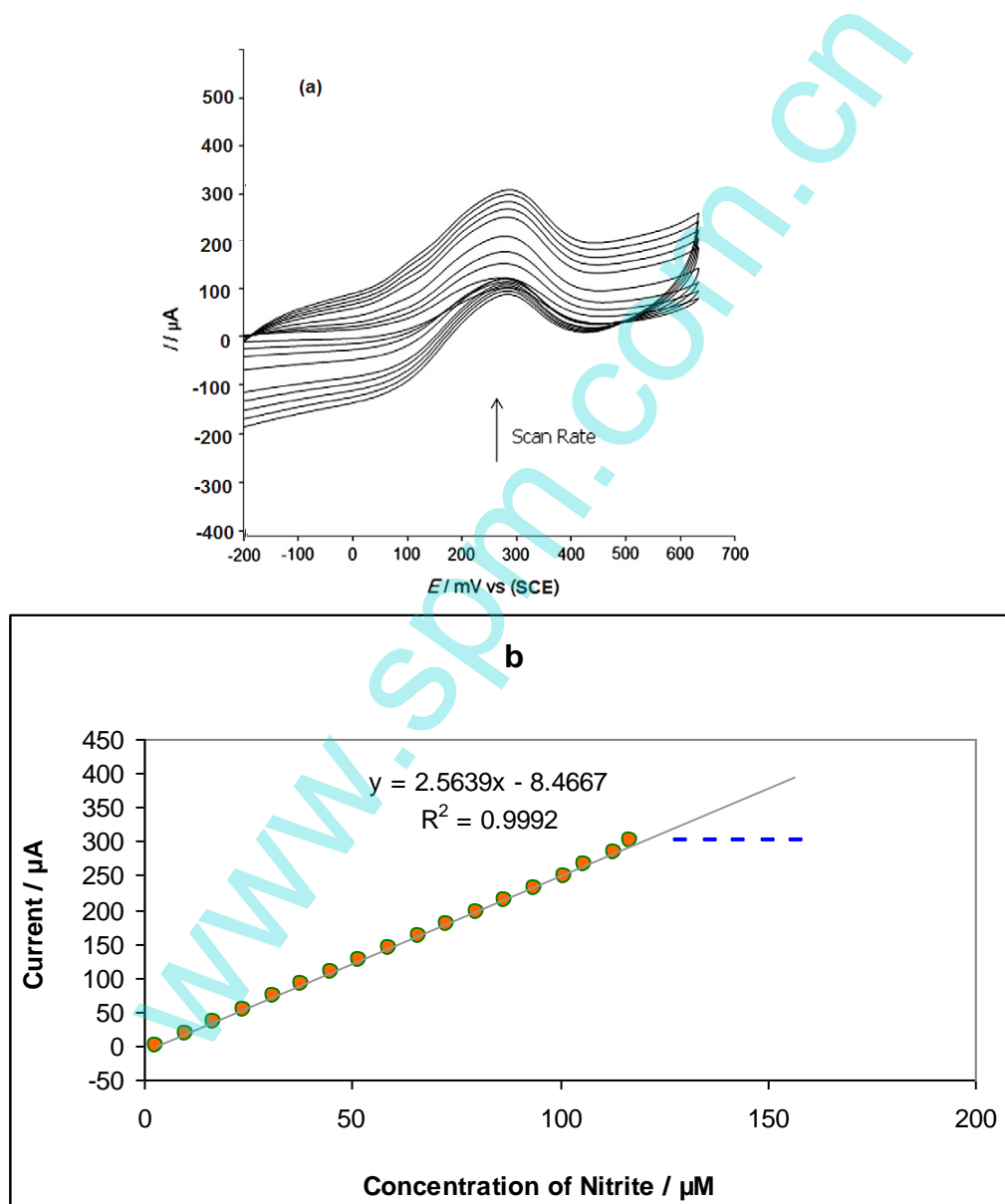


Figure 6. (a) Cyclic voltammograms obtained at an HAO / ZrO_2 NPs/CPE electrode in 0.1M phosphate buffer solution (pH 7.0) for different concentrations of and (b) the relationship between anodic peak current of Hydroxylamine oxidase and different concentrations of NO_2^- (scan rate: 100 mVs^{-1}).

Upon the addition of an aliquot of NO_2^- to the buffer solution, the oxidation current increased steeply to reach a stable value (Fig 6 b). This implies the electrocatalytic property of electrode. Thus, this experiment has introduced a new biosensor for the sensitive determination of NO_2^- in solution and also the determination of Hydroxylamine at surface of working electrode (here CPE) ; in figure 6. (a), Cyclic voltammograms was obtained at an HAO / ZrO_2 NPs/CPE in 0.1M phosphate buffer solution (pH 7.0) for different concentrations and Figure 6. (b) Shows the relationship between anodic peak current of Hydroxylamine oxidase and different concentrations of NO_2^- (scan rate: 100 mVs^{-1}).

3.6. Stability of biosensor

The stability of HAO / ZrO_2 NPs/CPE electrode biosensor has been checked by carrying out experiments at the regular interval of a week and it has been found that HAO / ZrO_2 NPs/CPE electrode based biosensor retains its 87% activity after 21 days. The loss in the activity of biosensor is not resulted from the denaturation of Hydroxylamine oxidase, but it is raised from the poor adhesion of ZrO_2 Nanoparticles on the carbon paste electrode that we will found a solution for this problem in next researches. AS a result, interface materials have not high effect on operation of this biosensor.

4. CONCLUSION

The presented study led to open new reagents that are very suitable and applicable in biosensors. The use of HAO enzyme structure, ZrO_2 nanoparticles and electrochemical devices were very handy for us. The designed biosensor has many applications in medical and industrial studies; because the interface materials have not high effect on operation of this biosensor and it was very stable and very cheap to design.

References

1. J.M. Cooper, K.R. Greenough, C.J. McNeil, *J. Electroanal. Chem.* 347 (1993) 267.
2. G. Zhao, Z. Yin, L. Zhang, X. Wei, *Electrochem. Commun.*, 7 (2005) 256.
3. C. M. Welch, C. E. Banks, *Anal. Bioanal. Chem.*, 12 (2005) 382.
4. Lu, Z.; Huang, Q.; Rusling, J.-F. *J. Electroanal. Chem.*, 59 (1997) 423.
5. M. Mohammadian, L. Farzampannah, A. Behtash-oskouie, S. Majdi, G. Mohseni, M. Imandar, M. Shirzad, R. Soleimani, M. Negahdary. *Int. J. Electrochem. Sci.*, 8 (2013) 11215.
6. M.H. Pournaghi-Azar, H. Dastangoo. *J. Electroanal. Chem.*, 567, (2004), 211.
7. Antariksh Saxena, R.M. Tripathi, R. P. Singh, *DJNB*, 5 (2010) 427.
8. P. Mohanpuria, K. N. Rana, S. K. Yadav, *JNR.*, 10 (2008) 507.
9. J.L. Willit, E.F. Bowden, *J. Phys. Chem.* 94 (1990) 8241.
10. S Rezaei-Zarchi, M Negahdary, M Doroudian, M Hashemi, S Imani, N Rousta, A ... *Adv. Environ. Biol*, 5 (10), 3241-3248
11. M Negahdary, A Asadi, S Mehrtashfar, M Imandar, H Akbari-Dastjerdi, F Salahi, *Int J Electrochem Sci*, 7 (2012), 5185-5194

12. M Negahdary, S Rad, MT Noughabi, A Sarzaem, SP Noughabi, F Mirzaeinasab, *Adv.Stu. Bio*, 4 (3), 103-118
13. M Negahdary, MT Noughabi, E Rezaei, M Mazdapour, A Farasat, T Arabnezhad, *Adv. Environ. Biol*, 6 (3), 1095-1103
14. S Banapour, M Mazdapour, Z Dinpazhooh, F Salahi, MT Noughabi, M Negahdary, *Adv.Stu. Bio*, 4 (5), 231-243
15. M Negahdary, M Imandar, M Fazilati, M Mazdapour, M Ajdary, *J. Appl. Environ. Biol. Sci* 2 (8), 409-415.
16. Farough Salimi, Masoud Negahdary, Gholamreza Mazaheri, *Int. J. Electrochem. Sci* 7 (8) 7225-7234.
17. Gholamreza Mohseni, Masoud Negahdary, *Int J Electrochem Sci*, 7 (8) 7033-7044
18. Masoud Negahdary, Seyedeh Anousheh Sadeghi, *Int. J. Electrochem. Sci*, 7 (7) 6059-6069
19. Gholamreza Mohseni, Masoud Negahdary, *Int. J. Electrochem. Sci*, 7 (12) 12098-12109
20. Koorosh Fooladsaz, Masoud Negahdary, *Int. J. Electrochem. Sci*, 7 (10) 9892-9908
21. Masoud Negahdary, Amir Habibi-Tamijani, Asadollah Asadi, Saeid Ayati, *Journal of Chemistry*, 2013 (1) 1.
22. Masoud Negahdary, Saeed Rezaei-Zarchi, *ISRN Biophysics*, 2012 (1) 4.
23. Masoud Negahdary, Gholamreza Mazaheri, *Int. J. Anal. Chem*, 2012 1 (1).
24. X. Yuan, F.M. Hawkridge, J.F. Chlebowski, *J. Electroanal. Chem.* 350 (1993) 29.
25. P. Bertrand, O. Mbarki, M. Asso, L. Blanchard, F. Guerleequin, M. Tegoni, *Biochemistry.*, 34 (1995) 11071.